Neutrophil myeloperoxidase diminishes the toxic effects and mortality induced by lipopolysaccharide

Laurent L Reber, Caitlin Gillis, Philipp Starkl, Friederike Jönsson, Riccardo Sibilano, Thomas Marichal, Nicolas Gaudenzio, Marion Bérard, Stephan Rogalla, Christopher H Contag, et al.

JEM

Neutrophil myeloperoxidase diminishes the toxic effects and mortality induced by lipopolysaccharide

Laurent L. Reber,[1,2,8,10]* Caitlin M. Gillis,[8,10]* Philipp Starkl,[1,2] Friederike Jönsson,[8,10] Riccardo Sibilano,[1,2] Thomas Marichal,[1,2] Nicolas Gaudenzio,[1,2] Marion Bérard,[9] Stephan Rogalla,[3,4] Christopher H. Contag,[3,4,5,6,7] Pierre Bruhns,[8,10]** and Stephen J. Galli[1,2,5]**

[1]Department of Pathology, [2]Sean N. Parker Center for Allergy and Asthma Research, [3]Department of Pediatrics, Division of Neonatology, [4]Molecular Imaging Program at Stanford, [5]Department of Microbiology and Immunology, [6]Department of Radiology, and [7]Department of Bioengineering, Stanford University School of Medicine, Stanford, CA 94305
[8]Department of Immunology, Unit of Antibodies in Therapy and Pathology and [9]Animalerie Centrale, Institut Pasteur, 75015 Paris, France
[10]Institut National de la Santé et de la Recherche Médicale, U1222, 75015 Paris, France

The Journal of Experimental Medicine

Neutrophils have crucial antimicrobial functions but are also thought to contribute to tissue injury upon exposure to bacterial products, such as lipopolysaccharide (LPS). To study the role of neutrophils in LPS-induced endotoxemia, we developed a new mouse model, *PMN*^{DTR} mice, in which injection of diphtheria toxin induces selective neutrophil ablation. Using this model, we found, surprisingly, that neutrophils serve to protect the host from LPS-induced lethal inflammation. This protective role was observed in conventional and germ-free animal facilities, indicating that it does not depend on a particular microbiological environment. Blockade or genetic deletion of myeloperoxidase (MPO), a key neutrophil enzyme, significantly increased mortality after LPS challenge, and adoptive transfer experiments confirmed that neutrophil-derived MPO contributes importantly to protection from endotoxemia. Our findings imply that, in addition to their well-established antimicrobial properties, neutrophils can contribute to optimal host protection by limiting the extent of endotoxin-induced inflammation in an MPO-dependent manner.

INTRODUCTION

Innate immune recognition of invading pathogens by pattern-recognition receptors (PRRs) is important to initiate protective immune responses (Medzhitov, 2007; Kawai and Akira, 2011). Yet uncontrolled activation of PRRs by pathogen-associated molecular patterns (PAMPs), such as LPS, can result in unbalanced cytokine production and potentially fatal tissue injury. Neutrophils express multiple PRRs, including the LPS receptor TLR4 (Hayashi et al., 2003), and are typically the first immune cells to be recruited to sites of infection (Kolaczkowska and Kubes, 2013; Mócsai, 2013; Mayadas et al., 2014; Nauseef and Borregaard, 2014). Neutrophils can efficiently kill bacteria through different defense mechanisms (Borregaard, 2010; Kolaczkowska and Kubes, 2013; Mócsai, 2013; Mayadas et al., 2014); however, some neutrophil products may be detrimental to the host, particularly in the context of excessive activation by PAMPs, such as during LPS-induced endotoxemia (Mócsai, 2013; Mayadas et al., 2014; Nauseef and Borregaard, 2014). Indeed, it is generally considered that neutrophils exacerbate the inflammation and tissue damage associated with LPS exposure. Surprisingly, there is a lack of formal evidence to demonstrate this detrimental role for neutrophils. Moreover, systemic inflammation leads to a functionally heterogeneous neutrophil compartment (Pillay et al., 2010) and, in humans, low-dose LPS exposure induces the appearance of a subset of CD62L^{dim}CD11b^{high} neutrophils that can suppress T cell activation ex vivo (Pillay et al., 2012). The latter finding suggests that some neutrophils might possess immunosuppressive functions in the context of endotoxemia.

In the present study, we used mouse models to investigate further the role of neutrophils during LPS-induced endotoxemia. There is a paucity of suitable models available to study neutrophil functions in vivo: animals with constitutive neutropenia exhibit other immune abnormalities and are more susceptible to infections (Hock et al., 2003), whereas antibodies used at high doses to deplete neutrophils have known or likely effects on other cell populations (Conlan and North, 1994; Daley et al., 2008). Therefore, we have devel-

*L.L. Reber and C.M. Gillis contributed equally to this paper.

**P. Bruhns and S.J. Galli contributed equally to this paper.

Correspondence to Stephen J. Galli: sgalli@stanford.edu; or Pierre Bruhns: bruhns@pasteur.fr

P. Starkl's present address is CeMM, Research Center for Molecular Medicine of the Austrian Academy of Sciences and Research Laboratory of Infection Biology, Dept. of Medicine I, Medical University of Vienna, 1090 Vienna, Austria.

T. Marichal's present address is GIGA-Research and Faculty of Veterinary Medicine, University of Liege, 4000 Liege, Belgium.

Abbreviations used: 4-ABAH, 4-aminobenzoic acid hydrazide; CLP, cecal ligation and puncture; DT, diphtheria toxin; DTR, simian DT receptor; GF, germ free; GMP, granulocyte-macrophage progenitor; MPO, myeloperoxidase; PRR, pattern-recognition receptor; SPF, specific pathogen free.

The Rockefeller University Press $30.00
J. Exp. Med. 2017 Vol. 214 No. 5 1249–1258
https://doi.org/10.1084/jem.20161238

oped a new mouse model, which we call *PMN*^{DTR} mice, that allows selective and inducible ablation of neutrophils upon injection of diphtheria toxin (DT). Using this model, we discovered that, instead of exacerbating LPS-induced toxicity, neutrophils diminish the toxic effects and mortality induced by LPS in mice. We further demonstrated that this protective function is mediated by the major enzyme of neutrophils, myeloperoxidase (MPO).

RESULTS AND DISCUSSION

Antibody-mediated neutrophil depletion increases LPS-induced mortality

To evaluate the contribution of neutrophils to LPS-induced endotoxemia in mice, we first assessed the phenotype of mouse neutrophil activation after i.p. LPS administration. A marked dose-dependent decrease in expression of CD62L and increase in CD11b was observed in neutrophils from the blood (Fig. 1, A–C), peritoneal cavity, and BM (Fig. S1, A–D). This activated phenotype is consistent with the CD62L^{dim}CD11b^{high} subset of blood neutrophils observed after injection of low-dose LPS in humans, which display immunosuppressive characteristics ex vivo (Pillay et al., 2012). We then assessed the role of neutrophils in the LPS-induced endotoxemia model using neutrophil-depleting antibodies. Neutrophil depletion by treatment with anti–Gr-1 or anti-Ly6G antibodies greatly increased the hypothermia and mortality induced by LPS injection (Fig. 1, D–G). Despite the development of considerable neutrophilia in mice treated with isotype control antibodies, mice treated with neutrophil-depleting antibodies remained neutropenic after LPS injection (Fig. S1, E and F).

We obtained very similar results at both Stanford University and Institut Pasteur (Fig. 1, F and G vs. H). However, WT mice maintained at Institut Pasteur were more susceptible to LPS toxicity than mice at Stanford University (not depicted). Such a difference in LPS reactivity could reflect differences in the microbiological environment. Given the known impact of commensal bacteria on neutrophil functions (Zhang et al., 2015), we therefore compared responses to LPS and the effect of neutrophil depletion between mice housed in a conventional animal facility (specific pathogen free [SPF]) and those housed in a germ-free (GF) facility. We observed greatly reduced LPS-induced mortality in GF mice (Fig. 1, H and I), as described previously (Souza et al., 2004), yet depletion of neutrophils using an anti–Gr-1 antibody increased mortality in both SPF and GF mice, and responses of anti–Gr-1–treated SPF and GF mice were statistically indistinguishable (Fig. 1, H and I). Therefore, neutrophils appear to play a microorganism-independent role in limiting the extent of endotoxin-induced lethal shock.

Neutrophil-depleted mice were also more susceptible to endotoxemia at a 10-times-reduced dose of LPS (2.5 mg/kg; Fig. S1, G and I): this lower dose was fatal when administered to neutrophil-depleted mice, but not controls. On the other hand, when LPS (10 µg/kg) was given in the context of liver damage (by co-administration of the hepatotoxin D-galactosamine), we did not observe a difference in susceptibility of neutrophil-depleted mice compared with controls (Fig. S1, H and J). These findings indicate that neutrophil depletion renders mice more susceptible to both low- and high-dose systemic LPS administration. However, the apparent protective effect of neutrophils is not evident when LPS is given in a model of acute liver damage.

A new mouse model for selective and inducible ablation of neutrophils confirms that neutrophil depletion enhances susceptibility to endotoxemia and sepsis

Because the efficiency and selectivity of neutrophil-depleting antibodies is still a matter of debate (Daley et al., 2008; Wang et al., 2012; Nigrovic, 2013; Yipp and Kubes, 2013), we generated a new transgenic mouse model allowing selective and inducible ablation of neutrophils. We used MRP8-Cre mice expressing Cre recombinase under the control of the neutrophil-associated human MRP8 promoter, with an IRES-GFP reporter (Passegué et al., 2004; Elliott et al., 2011; Abram et al., 2013). First, we confirmed that GFP expression, as a marker of Cre activity, is restricted to neutrophils among major mature immune cell types in the blood, BM, spleen, and peritoneal lavage fluid (Fig. 2 A and Fig. S2 A). When crossed to ROSA-iEYFP^{KI} reporter mice, the MRP8 promoter was described to drive Cre-mediated deletion in 80–95% of neutrophils, with minor leakage (<20%) into some monocyte/macrophage populations (Abram et al., 2014), a finding we confirmed in the blood compartment (Fig. S2 B). We then crossed MRP8-Cre mice with ROSA-iDTR^{KI} mice, which bear a Cre-inducible simian DT receptor (DTR; Buch et al., 2005), to generate mice with DTR expression restricted to neutrophils. A single injection of DT had no effect in control mice (MRP8-Cre^{-}; ROSA-iDTR^{KI}, named hereafter *PMN*^{WT} mice) but markedly reduced neutrophil numbers in the blood, spleen, and BM of MRP8-Cre^{+}; ROSA-iDTR^{KI} (named hereafter *PMN*^{DTR}) mice at 24 h (Fig. 2, B–D; and Fig. S2 C). We found no significant effect of DT treatment on most of the other major immune cell types we assessed: B and T lymphocytes, platelets, eosinophils, basophils, dendritic cells, macrophages, and BM granulocyte-macrophage progenitors (GMPs; Fig. S2, E–H). Notably, however, we observed a significant reduction in the numbers of blood monocytes and the Ly6C^{hi} population of spleen monocytes in DT-treated *PMN*^{DTR} mice (Fig. S2, E and F), which is in accord with the data from MRP8-Cre^{+}; ROSA-iEYFP^{KI} mice, indicating that some Cre expression occurs in the monocyte compartment (Abram et al., 2014; Fig. S2 B). Consistent with a lack of effect of DT on GMPs, the neutrophil depletion in *PMN*^{DTR} mice was transient, and blood neutrophils started to reappear 2 d after DT injection (Fig. S2 D).

In accord with the results obtained with neutrophil-depleting antibodies (Fig. 1), we found that *PMN*^{DTR} mice were much more susceptible than *PMN*^{WT} mice to the development of hypothermia and death after LPS injection (Fig. 2, E and F). Despite considerable neutrophilia in

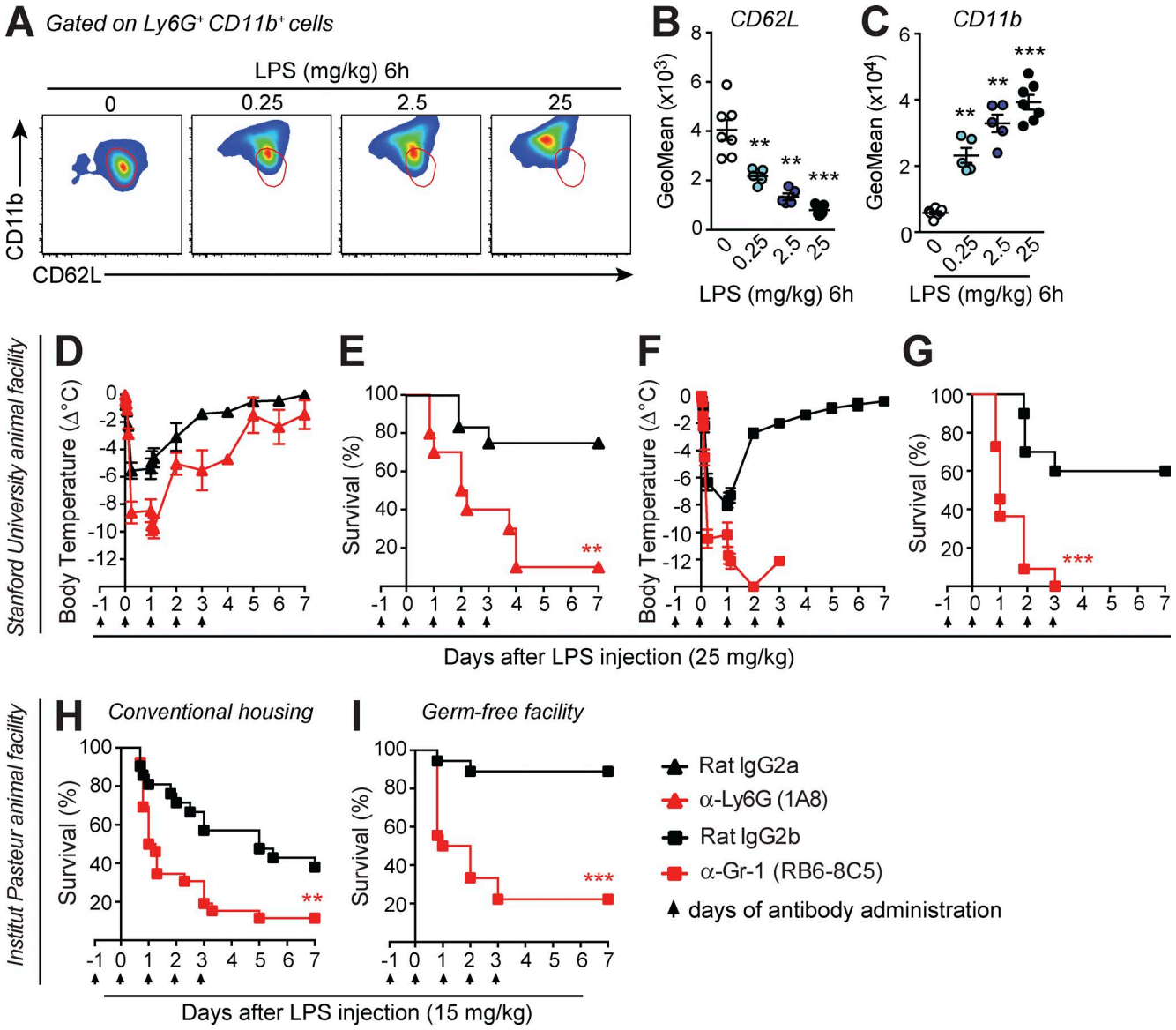

Figure 1. **Antibody-mediated neutrophil depletion results in increased mortality after LPS injection.** (A–C) Representative flow cytometry profile (A) and quantification of CD62L (B) and CD11b (C) by geometric mean fluorescence intensity (GeoMean) on Ly6G$^+$ CD11b$^+$ blood neutrophils 6 h after LPS injection at the indicated concentrations. Red areas outlined in A provide a visual indication of CD62L and CD11b on the neutrophil population from the control 0 group. B and C show values from individual mice; bars indicate means ± SEM pooled from two independent experiments. **, $P < 0.01$; ***, $P < 0.001$ versus control 0 group by two-tailed Mann–Whitney *U* test. (D–I) Changes in body temperature (Δ°C [mean ± SEM]) and survival (percentage of live animals) after LPS injection in C57BL/6J mice treated i.p. with anti-Ly6G (D and E), anti–Gr-1 (F–I) neutrophil-depleting antibodies, or respective isotype control antibodies. Data in D–G are pooled from three independent experiments performed at Stanford University (total n = 10–12/group). Data in H are pooled from three independent experiments performed in the Institut Pasteur conventional SPF animal facility (total n = 21–26/group). Data in I are pooled from two independent experiments performed in the Institut Pasteur GF animal facility (total n = 18/group). **, $P < 0.01$; ***, $P < 0.001$ versus the corresponding isotype control group by Mantel–Cox log-rank test. Arrows in D–I indicate days of i.p. injection of the neutrophil-depleting or isotype control antibodies.

PMN^{WT} mice, *PMN*^{DTR} mice remained deficient in neutrophils after LPS injection (Fig. 2 G). We found elevated levels of cytokines and chemokines in the blood 6 h after LPS injection in *PMN*^{DTR} mice compared with *PMN*^{WT} mice (Fig. 2, H–L), supporting a protective role for neutrophils in LPS-induced endotoxemia.

To validate *PMN*^{DTR} mice as a model to study neutrophils in vivo in an inflammatory context, we also assessed responses in the cecal ligation and puncture (CLP) model of polymicrobial sepsis (Fig. S2, I–M). Although CLP induced strong neutrophilia in *PMN*^{WT} mice, neutrophils remained barely detectable in the blood and peritoneal cavity of DT-

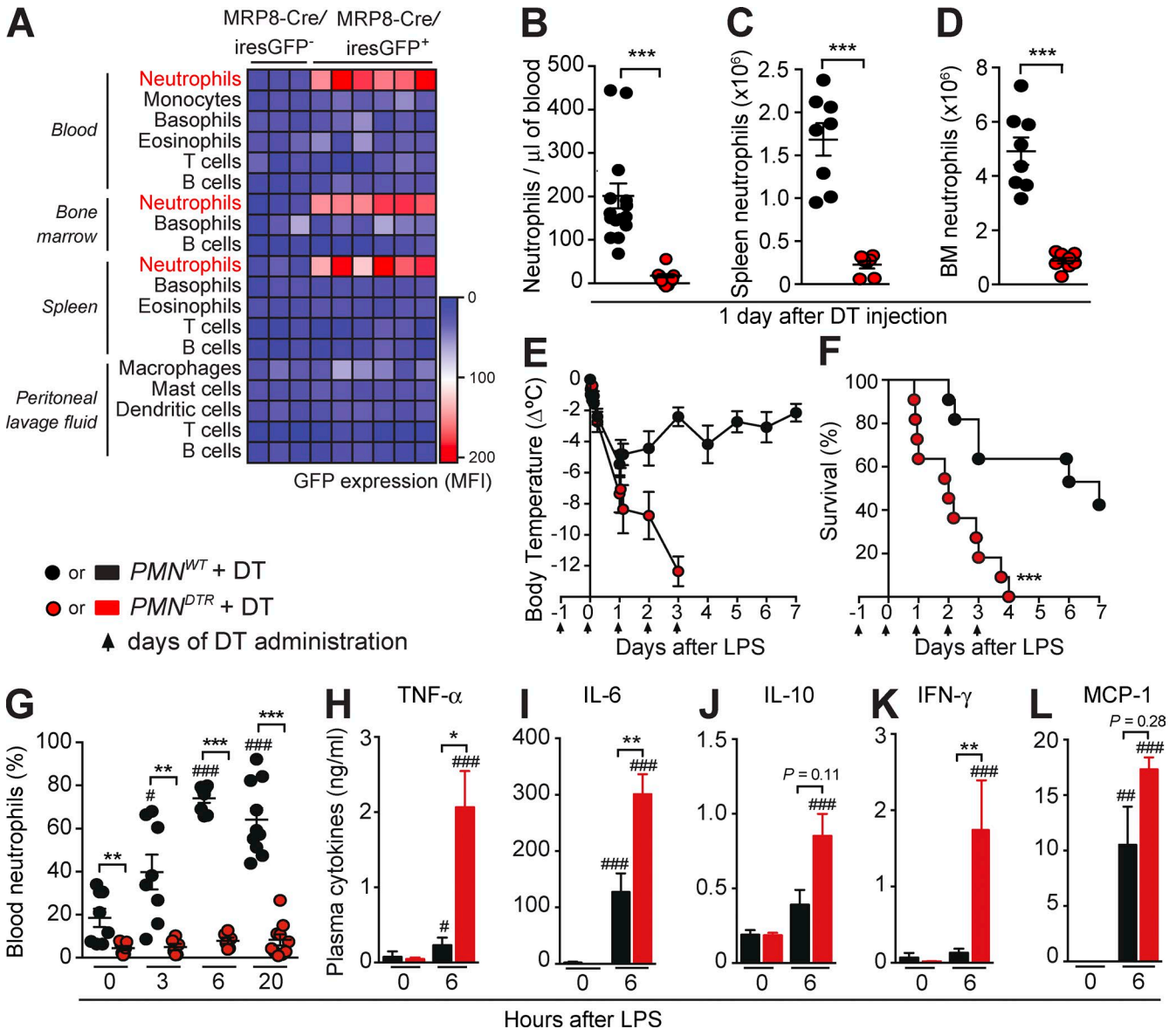

Figure 2. **Injection of DT in *PMN*^{DTR} mice induces marked depletion of neutrophils and enhances susceptibility to LPS-induced endotoxemia.** (A) GFP expression (mean fluorescence intensity [MFI]) among leukocytes in the blood, BM, spleen, and peritoneal lavage fluid of *MRP8-Cre/iresGFP*$^{+}$ mice and *MRP8-Cre/iresGFP*$^{-}$ littermate controls. Results in A are pooled from three independent experiments, each column representing data from one mouse. (B–D) Numbers of blood (B), spleen (C), and BM (D) neutrophils 24 h after i.p. injection of 500 ng DT into *PMN*^{DTR} mice and *PMN*^{WT} littermate control mice. Results in B–D show values from individual mice; bars indicate means ± SEM pooled from three (C and D; total n = 7–8/group) or four (B; total n = 15–16/group) independent experiments. (E and F) Changes in body temperature (Δ°C [mean ± SEM]; E) and survival (percentage of live animals; F) after LPS injection in DT-treated *PMN*^{DTR} and *PMN*^{WT} mice. Data in E and F are pooled from three independent experiments (total n = 11/group); arrows indicate days of i.p. injection of DT. (G) Percentage of blood neutrophils before (time 0) and 3, 6, and 20 h after LPS injection in DT-treated *PMN*^{DTR} mice and *PMN*^{WT} controls. Data show values from individual mice; bars indicate means ± SEM pooled from three independent experiments (n = 6–10/group). (H–L) Levels of TNF-α (H), IL-6 (I), IL-10 (J), IFN-γ (K), and MCP-1 (L) in the plasma of DT-treated *PMN*^{DTR} mice and *PMN*^{WT} littermate controls before (time 0) and 6 h after LPS injection (n = 6–16/group). Results in H–L are means ± SEM pooled from three independent experiments. *, P < 0.05; **, P < 0.01; ***, P < 0.001 versus *PMN*^{WT} group and $^{\#}$, P < 0.05; $^{\#\#}$, P < 0.01; $^{\#\#\#}$, P < 0.001 versus same group at time 0 by Mann–Whitney *U* test (B–D and G–L) or Mantel–Cox log-rank test (E and F).

treated *PMN*^{DTR} mice (Fig. S2 L). Confirming the critical role of neutrophils in defense against bacteria, we found that DT-treated *PMN*^{DTR} mice had diminished survival after CLP compared with DT-treated *PMN*^{WT} mice (Fig. S2 I), with greater numbers of bacteria in the blood and peritoneal cavity (Fig. S2, J and K) and elevated levels of cytokines and chemokines in the blood, 18 h after CLP (Fig. S2 M). Thus, *PMN*^{DTR} mice represent a valuable model for studying neu-

trophils during in vivo inflammation and confirm a protective role for neutrophils in LPS-induced endotoxemia and CLP-mediated polymicrobial sepsis.

MPO plays a beneficial role during sepsis and endotoxemia

MPO is the major enzyme produced by neutrophils and has an antibacterial function in sepsis (Klebanoff, 2005). A recent study indicated that diminished MPO expression might be a good predictor for identifying septic shock patients at high risk of death (Demaret et al., 2015). We therefore hypothesized that, in addition to its antimicrobial properties, MPO might contribute to the beneficial function of neutrophils during LPS-induced endotoxemia. We first confirmed that MPO-deficient mice have increased mortality, elevated levels of blood cytokines and chemokines, and higher bacterial burden in the CLP model (Gaut et al., 2001; Fig. S3, A–E). We then assessed responses of $Mpo^{-/-}$ mice in the LPS-induced endotoxemia model. Circulating neutrophils from MPO-deficient animals acquired a $CD62L^{dim}CD11b^{high}$ phenotype similar to that of MPO-sufficient animals 6 h after injection of LPS (Fig. 3 A and Fig. S3 F). However, $Mpo^{-/-}$ mice developed significantly increased hypothermia and mortality in response to LPS compared with WT mice (Fig. 3, B and C), as well as elevated blood levels of cytokines and chemokines, despite similar levels of neutrophils in the blood (Fig. S3, G and H). Furthermore, treatment of WT mice with the MPO inhibitor 4-aminobenzoic acid hydrazide (4-ABAH; Kettle et al., 1995; Gross et al., 2009; Zhang et al., 2013) significantly increased mortality in response to LPS, supporting a protective role for MPO during endotoxemia (Fig. 3 D).

Although several myeloid cell types can produce MPO, including neutrophils, monocytes, and macrophages, we found that MPO levels in the peritoneal cavity were reduced by 70% in neutrophil-depleted PMN^{DTR} mice compared with PMN^{WT} mice 6 h after LPS injection (Fig. 3 E). Using ex vivo bioluminescent imaging of MPO activity after Luminol administration (Gross et al., 2009; Zhang et al., 2013), we found that MPO activity was increased in the spleen and liver of both WT and PMN^{WT} mice after LPS, compared with PBS-treated controls (Fig. 3, F, G, and I). The pronounced MPO activity detected in the lungs was comparable between PBS- and LPS-treated mice (Fig. 3, H and I). MPO activity was markedly reduced in both $Mpo^{-/-}$ and PMN^{DTR} mice in all of the organs we examined and was statistically indistinguishable between MPO-deficient and neutrophil-deficient animals (Fig. 3, F–I; and Fig. S3 I), suggesting that neutrophils are the major source of MPO after LPS injection in vivo.

Finally, we performed adoptive transfer experiments to assess directly the importance of neutrophil-derived MPO during LPS endotoxemia. As a control, we first tested the efficiency of neutrophil engraftment in neutrophil-depleted PMN^{DTR} mice or PMN^{WT} controls using purified YFP^{+} neutrophils (isolated from the BM of MRP8-Cre^{+}; ROSA-$iEYFP^{KI}$ mice). We found significantly more circulating YFP^{+} neutrophils in the blood of PMN^{DTR} mice compared with PMN^{WT} mice 4 h after engraftment, indicating that PMN^{DTR} mice (in which endogenous neutrophils are depleted) represent an attractive model for adoptive transfer experiments (Fig. S3, J–L). We then engrafted PMN^{DTR} mice with neutrophils purified from either WT mice (WT PMNs → PMN^{DTR}) or $Mpo^{-/-}$ mice ($Mpo^{-/-}$ PMNs → PMN^{DTR}). LPS-induced hypothermia and survival in WT PMNs → PMN^{DTR} mice were similar to those observed in neutrophil-sufficient PMN^{WT} mice (Fig. 3, J and K). In contrast, $Mpo^{-/-}$ PMNs → PMN^{DTR} mice experienced significantly greater hypothermia and mortality compared with either WT PMNs → PMN^{DTR} mice or PMN^{WT} mice, and the responses in $Mpo^{-/-}$ PMNs → PMN^{DTR} mice were statistically indistinguishable from those of PMN^{DTR} mice not engrafted with neutrophils (Fig. 3, J and K). Thus, the adoptive transfer of MPO-sufficient, but not MPO-deficient, neutrophils ameliorated LPS-induced hypothermia and enhanced survival of neutrophil-depleted mice. Collectively, our data indicate that the protective function of neutrophils during endotoxemia is dependent, at least in part, on their major enzyme MPO.

Given the short half-life of adoptively transferred neutrophils, it is likely that the protective function of neutrophils and MPO in this endotoxemia model occurs early after exposure to LPS. In agreement with this, we observed markedly enhanced hypothermia in neutrophil-depleted mice and MPO-deficient mice compared with their respective controls as early as 3–6 h after injection of LPS (Fig. 1, D and F; and Fig. 3 B). In addition, mortality rates were already much higher at 15 h in both neutrophil-depleted and MPO-deficient mice compared with controls (Fig. 1, E and G; and Fig. 3 C).

The mechanisms by which neutrophil-derived MPO is protective during endotoxemia may be intrinsically MPO-dependent and/or secondary to phenotypic or functional alterations in neutrophils. MPO has been reported to bind to and activate neutrophils, support cell adhesion, and prolong neutrophil survival, mainly via interactions with CD11b/CD18 integrins (Johansson et al., 1997; Lau et al., 2005; El Kebir et al., 2008) or by electrostatic interactions (Klinke et al., 2011). Through such effects, MPO may support appropriate neutrophil localization in response to changes induced by systemic endotoxin and therefore help to localize neutrophil regulatory functions. Neutrophil death is also thought to contribute importantly to the control and resolution of inflammation, and macrophage uptake of aging or apoptotic neutrophils can dampen the inflammatory responses of the macrophages themselves (Fadok et al., 1998; Poon et al., 2014). Indeed, the intraperitoneal injection of apoptotic neutrophils was found to protect mice during LPS-induced endotoxic shock via CD14-dependent macrophage uptake (Ren et al., 2008). In our hands, the transfer of $Mpo^{-/-}$ neutrophils did not restore survival during endotoxemia, which suggests that the protective effect of neutrophil transfer is not merely attributable to the transfer of cells that thereafter undergo apoptosis. Conversely, it is possible that, in the absence of MPO, alterations

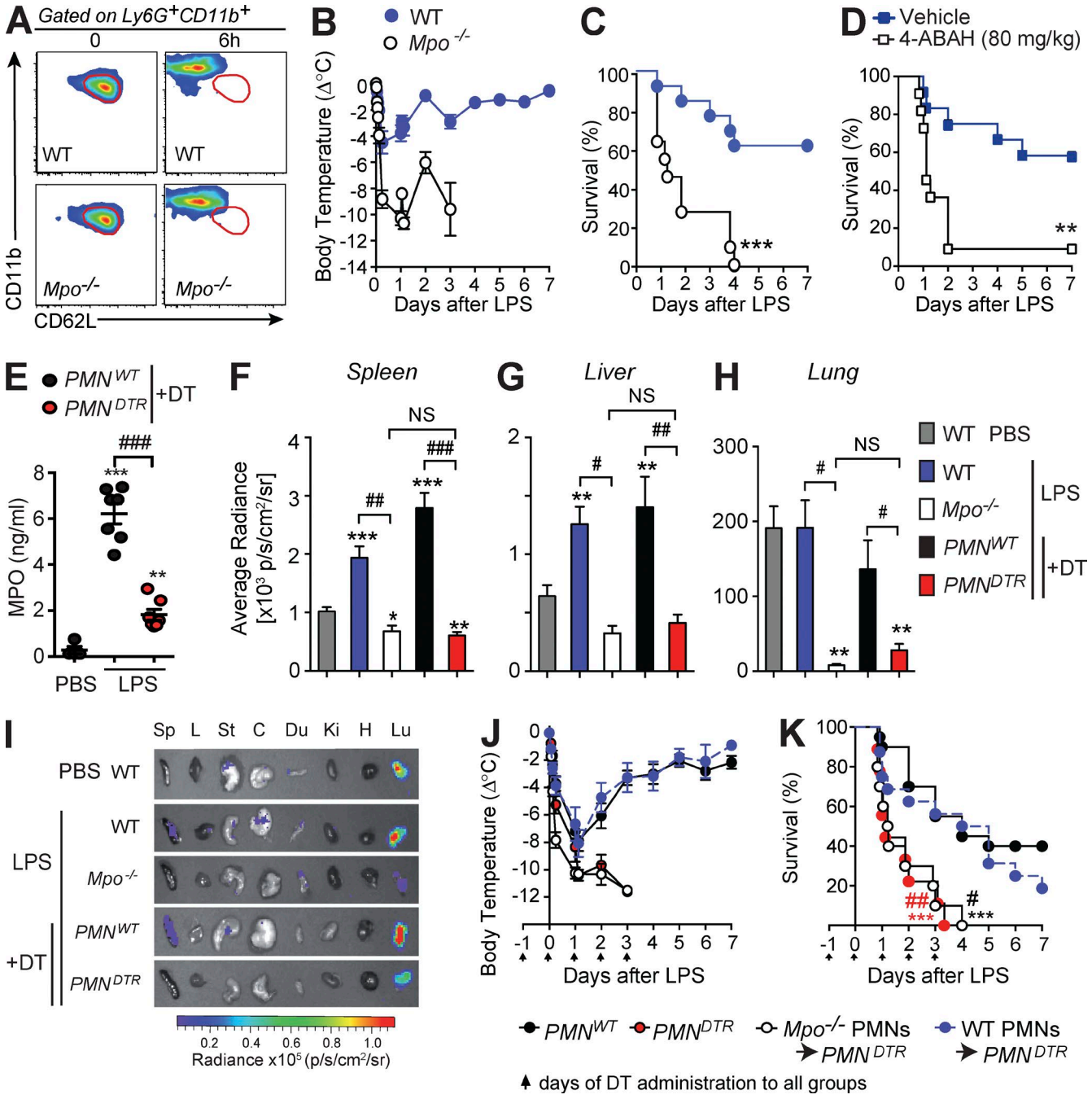

Figure 3. **Neutrophil-derived MPO diminishes LPS-induced hypothermia and mortality.** (A) Representative flow cytometry profile of Ly6G$^+$ CD11b$^+$ blood neutrophils 0 or 6 h after LPS injection in WT or *Mpo*$^{-/-}$ mice. Areas outlined in red indicate values for neutrophils from the control (time 0) group; data are representative of results obtained in two independent experiments. (B and C) Changes in body temperature (Δ°C [mean ± SEM]; B) and survival (percentage of live animals; C) after LPS injection in WT and *Mpo*$^{-/-}$ mice. (D) Survival after LPS injection in WT mice treated with the MPO inhibitor 4-ABAH or vehicle. Data in B–D are pooled from three independent experiments (total n = 11–13/group). **, P < 0.01; ***, P < 0.001 versus respective WT group (C) or vehicle-treated group (D) by Mantel–Cox log-rank test. (E) MPO in the peritoneal lavage fluid 6 h after injection with PBS (n = 4) or LPS (n = 7/group). Values from individual mice are shown; bars indicate means ± SEM pooled from two independent experiments. **, P < 0.01; ***, P < 0.001 versus PBS group and ###, P < 0.001 versus LPS-treated control group by unpaired Student's t test. (F–I) Bioluminescent visualization of MPO activity in various organs 6 h after injection of PBS or LPS in the indicated group. (F–H) Quantification of bioluminescence in spleen (F), liver (G), and lung (H). Data in F–H are means + SEM from three independent experiments (total n = 6–14/group) except for *Mpo*$^{-/-}$ mice (two independent experiments with a total of three to four mice). *, P < 0.05; **, P < 0.01; ***, P < 0.001 versus PBS-treated WT group and #, P < 0.05; ##, P < 0.01; ###, P < 0.001 versus corresponding LPS-treated control group by unpaired Student's t test. NS, not significant (P > 0.05). (I) Representative images of different organs (Sp, spleen; L, liver; St, stomach; C, cecum;

in neutrophil apoptosis might impair subsequent macrophage reprogramming and the induction of pro-resolution pathways.

In addition, it was recently reported that MPO can limit collateral tissue damage during antimicrobial oxidative bursts by converting diffusible and relatively long-lived H_2O_2 into highly reactive but locally confined HOCl (Schürmann et al., 2017). MPO-deficient mice exhibited increased H_2O_2 tissue levels during *Salmonella* infection, as well as increased lipid peroxidation and DNA damage. Although those authors described a local phenomenon occurring at the pathogen surface and in the surrounding tissues, it is possible that such anomalous reactive oxygen species generation and compartmentalization can also contribute, at least in part, to the exacerbated systemic inflammation that we observed in neutrophil- or MPO-deficient mice after LPS challenge. Intriguingly, MPO also can have antiinflammatory effects directly by its catalytic action, via the oxidative modification or destruction of soluble mediators of inflammation. Notable candidates include high-mobility group protein 1 (HMGB1), associated with lethality after endotoxin exposure (Wang et al., 1999) because the oxidative modification of HMGB1 determines its inflammatory effects (Venereau et al., 2012; Yang et al., 2013). MPO can catalyze the oxidation of lipid mediators, such as leukotrienes and prostaglandins (Zhang et al., 2002), and lipid peroxidation is a feature of systemic inflammation (Willenberg et al., 2016). Indeed, after endotoxin challenge, *Mpo*$^{-/-}$ mice were found to have elevated plasma levels of cysteinyl leukotrienes and reduced oxidative metabolites of arachidonic acid and linoleic acid (Kubala et al., 2010). Thus, MPO has the potential to systemically regulate the acute inflammatory response by modulating the formation of pro- and antiinflammatory lipid mediators.

Endotoxin challenge is a model of systemic inflammation relevant to our understanding of inflammatory pathways in multiple disease states: critically ill, post-trauma, or septic patients are characterized by severe systemic inflammation. Moreover, immune suppression is a secondary component of these conditions and is associated with poor patient outcome (Hotchkiss et al., 2013); "defective" neutrophil function is observed in such settings, although the heterogeneity of neutrophil subsets is rarely addressed (Pillay et al., 2010). Importantly, LPS exposure mimics the systemic immune activation that occurs during infection, yet decoupled from the presence of a pathogen. Here, we have identified an unexpected new role for neutrophils and neutrophil-derived MPO: enhancing innate host resistance to the toxic effects of LPS. Our results imply that, in addition to their direct antimicrobial functions, neutrophils and MPO can contribute to optimal host protection by modulating inflammation and limiting the toxic effects of endotoxins.

MATERIALS AND METHODS

Mice

C57BL/6J SPF (WT) mice were bred at the Stanford University Research Animal Facility or purchased from The Jackson Laboratory or Charles River and used for experiments after maintaining the mice for at least 1 wk in SPF conditions in either animal facility (Stanford or Pasteur). C57BL/6J GF mice were obtained from the Unit of Transgenesis, Archiving and Animal Models TAAM, UPS44, Orleans, France, or from Institut Pasteur and were maintained in sterile isolators at Institut Pasteur. ROSA-iDTR^{KI} mice (C57BL/6-*Gt(ROSA)26Sor*$^{tm1(HBEGF)Awai}$/J) were purchased from The Jackson Laboratory. *MRP8-Cre*$^{+}$ mice (B6.Cg-*Tg(S100A8-cre,-EGFP)1Ilw/J*) were obtained from I. Weissman (Stanford University, Stanford, CA) and C. Lowell (University of California San Francisco, San Francisco, CA). *MRP8-Cre*$^{+}$ mice were crossed with ROSA-iDTR^{KI} mice to generate *PMN*^{DTR} mice (MRP8-Cre^{+}; ROSA-iDTR^{KI}) and *PMN*^{WT} littermate controls (MRP8-Cre^{-}; ROSA-iDTR^{KI}). ROSA-iEYFP^{KI} reporter mice (B6.129X1-*Gt(ROSA)26Sor*$^{tm1(EYFP)Cos}$/J) were obtained from G. Eberl (Institut Pasteur, Paris, France) and crossed with *MRP8-Cre*$^{+}$ mice to generate MRP8-Cre^{+}; iEYFP^{KI} mice with YFP-fluorescent neutrophils (Figs. S2 B and S3, J–L). *Mpo*$^{-/-}$ mice (B6.129X1-Mpotm1Lus/J) were purchased from The Jackson Laboratory and bred in the Institut Pasteur or Stanford University SPF Animal Facilities. We used age- and sex-matched mice for all experiments. All animal care and experimentation were conducted in compliance with the guidelines of the National Institutes of Health and with the specific approval of the Institutional Animal Care and Use Committees of Stanford University and the Animal Ethics committee (Institut Pasteur, Paris, France) registered under #C2EA-89.

DT- and antibody-mediated ablation of neutrophils

PMN^{DTR} mice and *PMN*^{WT} littermate control mice were injected i.p. with 500 ng DT (Sigma-Aldrich). For antibody-mediated neutrophil depletion, WT mice were injected i.p. with anti-Ly6G (clone 1A8, 500 µg), anti-Gr-1 (clone RB6-8C5, 300 µg) or respective isotype control antibodies (rat IgG2a clone 2A3 or rat IgG2b clone LTF-2). Injections were performed in 200 µl PBS commencing 1 d before challenge; additional injections were performed 2 h before LPS injection or CLP and daily thereafter. The RB6-8C5 anti-

Du, duodenum; Ki, kidney; H, heart; and L, lung). (J and K) Changes in body temperature (J) and survival (K) after LPS injection in DT-treated *PMN*^{DTR} mice ($n = 9$), *PMN*^{WT} littermate controls ($n = 24$), and *PMN*^{DTR} mice engrafted i.v. with 10^7 purified BM neutrophils from WT mice (WT PMNs → *PMN*^{DTR}; $n = 16$) or from *Mpo*$^{-/-}$ mice (*Mpo*$^{-/-}$ PMNs → *PMN*^{DTR}; $n = 10$); arrows indicate days of i.p. injection of DT. Data are pooled from two (*Mpo*$^{-/-}$ PMNs → *PMN*^{DTR} group), three (*PMN*^{DTR} group), or five (*PMN*^{WT} and WT PMNs → *PMN*^{DTR} groups) independent experiments. ***, $P < 0.001$ versus *PMN*^{WT} group and $^{\#}$, $P < 0.05$; $^{\#\#}$, $P < 0.01$ versus WT PMNs → *PMN*^{DTR} group by Mantel–Cox log-rank test.

bodies used at the Institut Pasteur (Fig. 1, H and I) were produced from hybridomas provided by R. Coffman (Dynavax Technologies, Berkeley, CA), and purified by Protein G affinity purification from hybridoma supernatants. All other antibodies were from Bio X Cell.

In vivo treatments

Mice were injected i.p. with LPS at 15 mg/kg (for the experiments performed at Institut Pasteur; Fig. 1, H and I), 25 mg/kg, or the indicated doses in 200 µl PBS (Fig. 1, A–C; and Fig. S1, A–D; *Escherichia coli*, serotype 055:B5; Sigma-Aldrich). Hypothermia was monitored, and mice were observed for mortality at least twice daily. Mice that were clearly moribund were euthanized. For experiments involving GF mice, treatments were performed in parallel between GF and SPF facilities at Institut Pasteur, and all solutions were prepared sterile. For pharmacological inhibition of MPO activity, mice were injected i.p. with 80 mg/kg MPO inhibitor 4-ABAH (Sigma-Aldrich; Zhang et al., 2013) 3 h before and 6, 24, and 36 h after challenge with LPS (Fig. 3 D).

Flow cytometry and blood cell analyses

We used flow cytometry to identify and enumerate immune cells in BM, peripheral blood, peritoneal lavage fluid, and spleen. In brief, red blood cells were lysed by treatment with pH 7.3 ACK lysis buffer (0.15 M NH_4Cl, 1 mM $KHCO_3$, and 0.1 mM EDTA, pH 8.0) or RBC lysis buffer (BD). Peritoneal lavages were performed with 2 ml of ice-cold PBS, and cells were washed and counted using a hemocytometer. In some experiments, cells were blocked with unconjugated anti-FcγRII/III (CD16/CD32) antibodies (Bio X Cell) on ice for 5 min. Cells were stained with a combination of antibodies on ice for 30 min. Immune cell populations were identified as follows: neutrophils ($CD11b^+/Gr\text{-}1^{high}$, $CD11b^+/Ly6G^+$, or $CD45^+/CD11b^+/Ly6G^+$), blood monocytes ($CD11b^+/Ly6G^-/CD115^+$ and $Ly6C^{hi}$ or $Ly6C^{low}$), spleen macrophages ($CD11b^{low/+}/F4/80^+$), spleen monocytes ($CD11b^+/F4/80^{low/-}/Ly6G^-/SSC^{low}$ and $Ly6C^{hi}$ or $Ly6C^{int}$) and monocyte-derived DCs ($CD11b^+/F4/80^{low/-}/Ly6G^-/SSC^{low}/Ly6C^{low}/CD11c^+$), macrophages in peritoneal lavage fluid ($CD11b^+/F4/80^+$), basophils ($CD49b^+/FcεRIα^+$), mast cells ($c\text{-}KIT^+/FcεRIα^+$), eosinophils ($CD11b^+$; $Siglec\text{-}F^+$; SSC^{high}), dendritic cells ($CD11c^+$), T cells ($CD3ε^+/B220^-$), and B cells ($CD3ε^-/B220^+$). For analysis of BM progenitor cells (Fig. S1), BM cells were stained with lineage markers (Gr-1, Ter119, CD4, CD8, CD3, B220, CD19), Sca-1, c-KIT, CD34, and FcγRII/III (CD16/32). BM progenitor cell populations were identified as follows: GMPs ($Lineage^-/c\text{-}KIT^+/Sca\text{-}1^-/CD34^+/FcγRII/III^{high}$), common myeloid progenitors ($Lineage^-/c\text{-}KIT^+/Sca\text{-}1^-/CD34^+/FcγRII/III^{int}$), and megakaryocyte-erythrocyte progenitors ($Lineage^-/c\text{-}KIT^+/Sca\text{-}1^-/CD34^-/FcγRII/III^-$). Antibodies used were Gr-1 (RB6-8C5), Ly6C (AL21), Ly6G (1A8), CD11b (M1/70), F4/80 (BM8), FcεRIα (MAR-1), c-KIT (2B8), CD49b (DX5), Siglec-F (E50-2440), CD11c (N418), CD3ε (145-2C11), CD4 (RM4-5), CD8 (53–6.7), CD19 (6D5), CD34 (RAM34), CD45 (30F11), Sca-1 (D7), B220 (RA3-6B2), or CD62L (MEL-14). All antibodies were purchased from eBioscience, BD, Miltenyi Biotec, or BioLegend. Data were acquired using FACSCalibur, LSRII, Accuri C6 (all from BD), or MACSQuant (Miltenyi Biotec) flow cytometers. FITC channel was used for analysis of GFP or YFP expression (Fig. 2 A and Figs. S2 and S3). Data were analyzed with FlowJo software (Tree Star). Dead cells (identified by staining with propidium iodide or LIVE/DEAD Fixable Dead Cell Stains; Invitrogen) were not included in the analysis. For complete blood analysis (Fig. S2), total red blood cells, white blood cells, and platelets were counted using the Abbott Cell-Dyn 3500 automated hematology analyzer.

CLP

CLP was performed as described previously (Piliponsky et al., 2012). In brief, mice were deeply anesthetized by intramuscular injection of 100 mg/kg ketamine and 20 mg/kg xylazine, the cecum was exposed by a 1- to 2-cm midline incision on the anterior abdomen, and ligation of the distal half of the cecum and single puncture (with a 22-gauge needle) of the ligated segment were performed. The cecum was then placed back into the abdomen, 1 ml of sterile saline (pyrogen-free 0.9% NaCl) was administered into the peritoneal cavity, and the incision was closed using 9-mm steel wound clips. Mice were observed for mortality at least four times daily. Mice that were clearly moribund were euthanized by CO_2 inhalation.

Quantification of bacterial CFUs

Dilutions of peritoneal lavage fluids or blood were prepared, and samples were plated on lysogeny broth agar for peritoneal fluids or tryptose blood agar (BD), respectively. Colonies were counted after overnight incubation at 37°C.

Quantification of cytokines and chemokines in plasma

Levels of selected cytokines and chemokines in mouse plasma were analyzed by Cytometric Bead Array (mouse inflammation CBA kit; BD) and quantified using an Accuri C6 flow cytometer (BD).

Measurements of MPO and MPO activity

MPO was quantified from peritoneal lavage fluid by ELISA according to the manufacturer's instructions (R&D Systems). Bioluminescent imaging of MPO activity was performed 6 h after LPS injection (Zhang et al., 2013). Mice were anesthetized (isoflurane inhalation), and 10 min after injection of luminol-R (a mixture of Luminol [200 mg/kg; Sigma-Aldrich] and near-infrared quantum dots [QD800 from Life Sciences; 100 pmol]; 100 µl each i.p. + i.v.), animals were sacrificed and organs were sampled for imaging (2 min; open filter). Imaging and analysis was performed using an IVIS Spectrum with LivingImage software (Xenogen Product from PerkinElmer). We controlled for the in vivo distribution of luminol-R by fluorescent imaging of QD800 particles (ex-

citation 745 nm, emission 800 nm) and found no difference in fluorescence intensity between organs from LPS-treated neutrophil-sufficient and neutrophil-depleted mice or LPS-treated WT and *Mpo*$^{-/-}$ mice.

Adoptive transfer of neutrophils

BM neutrophils were purified from the tibia and femur by negative selection using the EasySep Mouse Neutrophil Enrichment kit (STEMCELL Technologies; >90% Gr-1$^+$ CD11b$^+$ and Ly-6G$^+$ CD11b$^+$ on average). Neutrophils (10^7 cells in Fig. 3 [J and K] and 2–10 × 10^6 in Fig. S3 [J–L]) were transferred i.v. (20–30 min before LPS injection; Fig. 3, J and K).

Statistical analyses

Data are presented as mean ± SEM. Data were analyzed for statistical significance using Mantel–Cox log-rank test, unpaired Mann–Whitney *U* test, or unpaired Student's *t* test, as indicated in figure legends. P-values <0.05 are considered statistically significant.

Online supplemental material

Fig. S1 contains data pertaining to the phenotype of neutrophils after LPS treatment and the effect of neutrophil depletion in endotoxemia induced by low-dose LPS or LPS/D-galactosamine. Fig. S2 shows the analysis of GFP expression in MRP8-Cre/IRES-GFP mice, the effect of DT treatment on other cell populations in *PMN*^{DTR} mice, and the responses of DT-treated *PMN*^{DTR} mice in the CLP model of sepsis. Fig. S3 shows the responses of MPO-deficient mice in the CLP model of sepsis and LPS-induced endotoxemia, the systemic quantification of MPO-induced bioluminescence, and the levels of neutrophils after adoptive transfer in *PMN*^{WT} versus *PMN*^{DTR} mice.

ACKNOWLEDGMENTS

We thank Irving Weissman and Clifford Lowell for sharing MRP8-Cre mice and Gerard Eberl for ROSA-EYFP reporter mice. We thank members of the Centre de Gnotobiologie de l'Institut Pasteur Murine, Institut Pasteur, for experiments with GF mice and animal husbandry. We also thank all members of the Galli and Bruhns laboratories for discussions and technical assistance.

L.L. Reber acknowledges support from the National Institutes of Health (grant K99AI110645), the European Commission (Marie Skłodowska-Curie Individual Fellowship H2020-MSCA-IF-2014 656086), and the Institut National de la Santé et de la Recherche Médicale (INSERM). C.M. Gillis was supported partly by a stipend from the Pasteur-Paris University (PPU) International PhD program and the Institut Carnot Pasteur Maladies Infectieuses, and partly by the Balsan company, as well as the European Research Council Seventh Framework Programme (ERC-2013-CoG 616050). P. Starkl was supported by a Max Kade Fellowship of the Max Kade Foundation and the Austrian Academy of Sciences and a Schroedinger Fellowship of the Austrian Science Fund (FWF; J3399-B21) and is supported by a European Commission Marie Skłodowska-Curie Individual Fellowship (H2020-MSCA-IF-2014 655153). F. Jönsson is an employee of the Centre National de la Recherche Scientifique. R. Sibilano was supported by the Lucile Packard Foundation for Children's Health and the Stanford University National Institutes of Health/National Center for Research Resources CTSA award (number UL1 RR025744). T. Marichal was supported by the European Commission Marie Curie International Outgoing Fellowship for Career Development (299954), is supported by the Acteria Foundation, and is a Research Associate of the Fonds De La Recherche Scientifique-FNRS. N. Gaudenzio was the recipient of a fellowship from the French Fondation pour la Recherche Médicale. S. Rogalla was supported in part by the George Will Foundation. C.H. Contag acknowledges support from the Child Health Research Institute at Stanford University and a generous gift from the Chambers Family Foundation for Excellence in Pediatric Research. P. Bruhns acknowledges support from the Institut Pasteur, the INSERM, the European Research Council Seventh Framework Programme (ERC-2013-CoG 616050), and the European Commission Horizon 2020 Framework Programme European Cooperation in Science and Technology (COST) Action BM1404 Mye-EUNITER. S.J. Galli acknowledges support from National Institutes of Health (grants AI023990, CA072074, AI070813, AR067145, U19 AI104209, and NS 080062), the Tobacco-Related Disease Research Program at the University of California, and the Department of Pathology, Stanford University School of Medicine.

The authors declare no competing financial interests.

Submitted: 2 August 2016
Revised: 30 January 2017
Accepted: 1 March 2017

REFERENCES

Abram, C.L., G.L. Roberge, L.I. Pao, B.G. Neel, and C.A. Lowell. 2013. Distinct roles for neutrophils and dendritic cells in inflammation and autoimmunity in motheaten mice. *Immunity.* 38:489–501. http://dx.doi.org/10.1016/j.immuni.2013.02.018

Abram, C.L., G.L. Roberge, Y. Hu, and C.A. Lowell. 2014. Comparative analysis of the efficiency and specificity of myeloid-Cre deleting strains using ROSA-EYFP reporter mice. *J. Immunol. Methods.* 408:89–100. http://dx.doi.org/10.1016/j.jim.2014.05.009

Borregaard, N. 2010. Neutrophils, from marrow to microbes. *Immunity.* 33:657–670. http://dx.doi.org/10.1016/j.immuni.2010.11.011

Buch, T., F.L. Heppner, C. Tertilt, T.J. Heinen, M. Kremer, F.T. Wunderlich, S. Jung, and A. Waisman. 2005. A Cre-inducible diphtheria toxin receptor mediates cell lineage ablation after toxin administration. *Nat. Methods.* 2:419–426. http://dx.doi.org/10.1038/nmeth762

Conlan, J.W., and R.J. North. 1994. Neutrophils are essential for early anti-Listeria defense in the liver, but not in the spleen or peritoneal cavity, as revealed by a granulocyte-depleting monoclonal antibody. *J. Exp. Med.* 179:259–268. http://dx.doi.org/10.1084/jem.179.1.259

Daley, J.M., A.A. Thomay, M.D. Connolly, J.S. Reichner, and J.E. Albina. 2008. Use of Ly6G-specific monoclonal antibody to deplete neutrophils in mice. *J. Leukoc. Biol.* 83:64–70. http://dx.doi.org/10.1189/jlb.0407247

Demaret, J., F. Venet, A. Friggeri, M.A. Cazalis, J. Plassais, L. Jallades, C. Malcus, F. Poitevin-Later, J. Textoris, A. Lepape, and G. Monneret. 2015. Marked alterations of neutrophil functions during sepsis-induced immunosuppression. *J. Leukoc. Biol.* 98:1081–1090. http://dx.doi.org/10.1189/jlb.4A0415-168RR

El Kebir, D., L. József, W. Pan, and J.G. Filep. 2008. Myeloperoxidase delays neutrophil apoptosis through CD11b/CD18 integrins and prolongs inflammation. *Circ. Res.* 103:352–359. http://dx.doi.org/10.1161/01.RES.0000326772.76822.7a

Elliott, E.R., J.A. Van Ziffle, P. Scapini, B.M. Sullivan, R.M. Locksley, and C.A. Lowell. 2011. Deletion of Syk in neutrophils prevents immune complex arthritis. *J. Immunol.* 187:4319–4330. http://dx.doi.org/10.4049/jimmunol.1100341

Fadok, V.A., D.L. Bratton, A. Konowal, P.W. Freed, J.Y. Westcott, and P.M. Henson. 1998. Macrophages that have ingested apoptotic cells in vitro inhibit proinflammatory cytokine production through autocrine/paracrine mechanisms involving TGF-beta, PGE2, and PAF. *J. Clin. Invest.* 101:890–898. http://dx.doi.org/10.1172/JCI1112

Gaut, J.P., G.C. Yeh, H.D. Tran, J. Byun, J.P. Henderson, G.M. Richter, M.L. Brennan, A.J. Lusis, A. Belaaouaj, R.S. Hotchkiss, and J.W. Heinecke. 2001. Neutrophils employ the myeloperoxidase system to generate antimicrobial brominating and chlorinating oxidants during sepsis. *Proc.*

Natl. Acad. Sci. USA. 98:11961–11966. http://dx.doi.org/10.1073/pnas.211190298

Gross, S., S.T. Gammon, B.L. Moss, D. Rauch, J. Harding, J.W. Heinecke, L. Ratner, and D. Piwnica-Worms. 2009. Bioluminescence imaging of myeloperoxidase activity in vivo. *Nat. Med.* 15:455–461. http://dx.doi.org/10.1038/nm.1886

Hayashi, F., T.K. Means, and A.D. Luster. 2003. Toll-like receptors stimulate human neutrophil function. *Blood.* 102:2660–2669. http://dx.doi.org/10.1182/blood-2003-04-1078

Hock, H., M.J. Hamblen, H.M. Rooke, D. Traver, R.T. Bronson, S. Cameron, and S.H. Orkin. 2003. Intrinsic requirement for zinc finger transcription factor Gfi-1 in neutrophil differentiation. *Immunity.* 18:109–120. http://dx.doi.org/10.1016/S1074-7613(02)00501-0

Hotchkiss, R.S., G. Monneret, and D. Payen. 2013. Sepsis-induced immunosuppression: From cellular dysfunctions to immunotherapy. *Nat. Rev. Immunol.* 13:862–874. http://dx.doi.org/10.1038/nri3552

Johansson, M.W., M. Patarroyo, F. Oberg, A. Siegbahn, and K. Nilsson. 1997. Myeloperoxidase mediates cell adhesion via the alpha M beta 2 integrin (Mac-1, CD11b/CD18). *J. Cell Sci.* 110:1133–1139.

Kawai, T., and S. Akira. 2011. Toll-like receptors and their crosstalk with other innate receptors in infection and immunity. *Immunity.* 34:637–650. http://dx.doi.org/10.1016/j.immuni.2011.05.006

Kettle, A.J., C.A. Gedye, M.B. Hampton, and C.C. Winterbourn. 1995. Inhibition of myeloperoxidase by benzoic acid hydrazides. *Biochem. J.* 308:559–563. http://dx.doi.org/10.1042/bj3080559

Klebanoff, S.J. 2005. Myeloperoxidase: Friend and foe. *J. Leukoc. Biol.* 77:598–625. http://dx.doi.org/10.1189/jlb.1204697

Klinke, A., C. Nussbaum, L. Kubala, K. Friedrichs, T.K. Rudolph, V. Rudolph, H.J. Paust, C. Schröder, D. Benten, D. Lau, et al. 2011. Myeloperoxidase attracts neutrophils by physical forces. *Blood.* 117:1350–1358. http://dx.doi.org/10.1182/blood-2010-05-284513

Kolaczkowska, E., and P. Kubes. 2013. Neutrophil recruitment and function in health and inflammation. *Nat. Rev. Immunol.* 13:159–175. http://dx.doi.org/10.1038/nri3399

Kubala, L., K.R. Schmelzer, A. Klinke, H. Kolarova, S. Baldus, B.D. Hammock, and J.P. Eiserich. 2010. Modulation of arachidonic and linoleic acid metabolites in myeloperoxidase-deficient mice during acute inflammation. *Free Radic. Biol. Med.* 48:1311–1320. http://dx.doi.org/10.1016/j.freeradbiomed.2010.02.010

Lau, D., H. Mollnau, J.P. Eiserich, B.A. Freeman, A. Daiber, U.M. Gehling, J. Brümmer, V. Rudolph, T. Münzel, T. Heitzer, et al. 2005. Myeloperoxidase mediates neutrophil activation by association with CD11b/CD18 integrins. *Proc. Natl. Acad. Sci. USA.* 102:431–436. http://dx.doi.org/10.1073/pnas.0405193102

Mayadas, T.N., X. Cullere, and C.A. Lowell. 2014. The multifaceted functions of neutrophils. *Annu. Rev. Pathol.* 9:181–218. http://dx.doi.org/10.1146/annurev-pathol-020712-164023

Medzhitov, R. 2007. Recognition of microorganisms and activation of the immune response. *Nature.* 449:819–826. http://dx.doi.org/10.1038/nature06246

Mócsai, A. 2013. Diverse novel functions of neutrophils in immunity, inflammation, and beyond. *J. Exp. Med.* 210:1283–1299. http://dx.doi.org/10.1084/jem.20122220

Nauseef, W.M., and N. Borregaard. 2014. Neutrophils at work. *Nat. Immunol.* 15:602–611. http://dx.doi.org/10.1038/ni.2921

Nigrovic, P.A. 2013. Response: Ly6G: A work in progress. *Blood.* 121:242–243. http://dx.doi.org/10.1182/blood-2012-10-459784

Passegué, E., E.F. Wagner, and I.L. Weissman. 2004. JunB deficiency leads to a myeloproliferative disorder arising from hematopoietic stem cells. *Cell.* 119:431–443. http://dx.doi.org/10.1016/j.cell.2004.10.010

Piliponsky, A.M., C.C. Chen, E.J. Rios, P.M. Treuting, A. Lahiri, M. Abrink, G. Pejler, M. Tsai, and S.J. Galli. 2012. The chymase mouse mast cell protease 4 degrades TNF, limits inflammation, and promotes survival in a model of sepsis. *Am. J. Pathol.* 181:875–886. http://dx.doi.org/10.1016/j.ajpath.2012.05.013

Pillay, J., B.P. Ramakers, V.M. Kamp, A.L. Loi, S.W. Lam, F. Hietbrink, L.P. Leenen, A.T. Tool, P. Pickkers, and L. Koenderman. 2010. Functional heterogeneity and differential priming of circulating neutrophils in human experimental endotoxemia. *J. Leukoc. Biol.* 88:211–220. http://dx.doi.org/10.1189/jlb.1209793

Pillay, J., V.M. Kamp, E. van Hoffen, T. Visser, T. Tak, J.W. Lammers, L.H. Ulfman, L.P. Leenen, P. Pickkers, and L. Koenderman. 2012. A subset of neutrophils in human systemic inflammation inhibits T cell responses through Mac-1. *J. Clin. Invest.* 122:327–336. http://dx.doi.org/10.1172/JCI57990

Poon, I.K., C.D. Lucas, A.G. Rossi, and K.S. Ravichandran. 2014. Apoptotic cell clearance: Basic biology and therapeutic potential. *Nat. Rev. Immunol.* 14:166–180. http://dx.doi.org/10.1038/nri3607

Ren, Y., Y. Xie, G. Jiang, J. Fan, J. Yeung, W. Li, P.K. Tam, and J. Savill. 2008. Apoptotic cells protect mice against lipopolysaccharide-induced shock. *J. Immunol.* 180:4978–4985. http://dx.doi.org/10.4049/jimmunol.180.7.4978

Schürmann, N., P. Forrer, O. Casse, J. Li, B. Felmy, A.V. Burgener, N. Ehrenfeuchter, W.D. Hardt, M. Recher, C. Hess, et al. 2017. Myeloperoxidase targets oxidative host attacks to *Salmonella* and prevents collateral tissue damage. *Nat. Microbiol.* 2:16268. http://dx.doi.org/10.1038/nmicrobiol.2016.268

Souza, D.G., A.T. Vieira, A.C. Soares, V. Pinho, J.R. Nicoli, L.Q. Vieira, and M.M. Teixeira. 2004. The essential role of the intestinal microbiota in facilitating acute inflammatory responses. *J. Immunol.* 173:4137–4146. http://dx.doi.org/10.4049/jimmunol.173.6.4137

Venereau, E., M. Casalgrandi, M. Schiraldi, D.J. Antoine, A. Cattaneo, F. De Marchis, J. Liu, A. Antonelli, A. Preti, L. Raeli, et al. 2012. Mutually exclusive redox forms of HMGB1 promote cell recruitment or proinflammatory cytokine release. *J. Exp. Med.* 209:1519–1528. http://dx.doi.org/10.1084/jem.20120189

Wang, H., O. Bloom, M. Zhang, J.M. Vishnubhakat, M. Ombrellino, J. Che, A. Frazier, H. Yang, S. Ivanova, L. Borovikova, et al. 1999. HMG-1 as a late mediator of endotoxin lethality in mice. *Science.* 285:248–251. http://dx.doi.org/10.1126/science.285.5425.248

Wang, J.X., A.M. Bair, S.L. King, R. Shnayder, Y.F. Huang, C.C. Shieh, R.J. Soberman, R.C. Fuhlbrigge, and P.A. Nigrovic. 2012. Ly6G ligation blocks recruitment of neutrophils via a β2-integrin-dependent mechanism. *Blood.* 120:1489–1498. http://dx.doi.org/10.1182/blood-2012-01-404046

Willenberg, I., K. Rund, S. Rong, N. Shushakova, F. Gueler, and N.H. Schebb. 2016. Characterization of changes in plasma and tissue oxylipin levels in LPS and CLP induced murine sepsis. *Inflamm. Res.* 65:133–142. http://dx.doi.org/10.1007/s00011-015-0897-7

Yang, H., D.J. Antoine, U. Andersson, and K.J. Tracey. 2013. The many faces of HMGB1: Molecular structure-functional activity in inflammation, apoptosis, and chemotaxis. *J. Leukoc. Biol.* 93:865–873. http://dx.doi.org/10.1189/jlb.1212662

Yipp, B.G., and P. Kubes. 2013. Antibodies against neutrophil LY6G do not inhibit leukocyte recruitment in mice in vivo. *Blood.* 121:241–242. http://dx.doi.org/10.1182/blood-2012-09-454348

Zhang, R., M.L. Brennan, Z. Shen, J.C. MacPherson, D. Schmitt, C.E. Molenda, and S.L. Hazen. 2002. Myeloperoxidase functions as a major enzymatic catalyst for initiation of lipid peroxidation at sites of inflammation. *J. Biol. Chem.* 277:46116–46122. http://dx.doi.org/10.1074/jbc.M209124200

SUPPLEMENTAL MATERIAL

Reber et al., https://doi.org/10.1084/jem.20161238

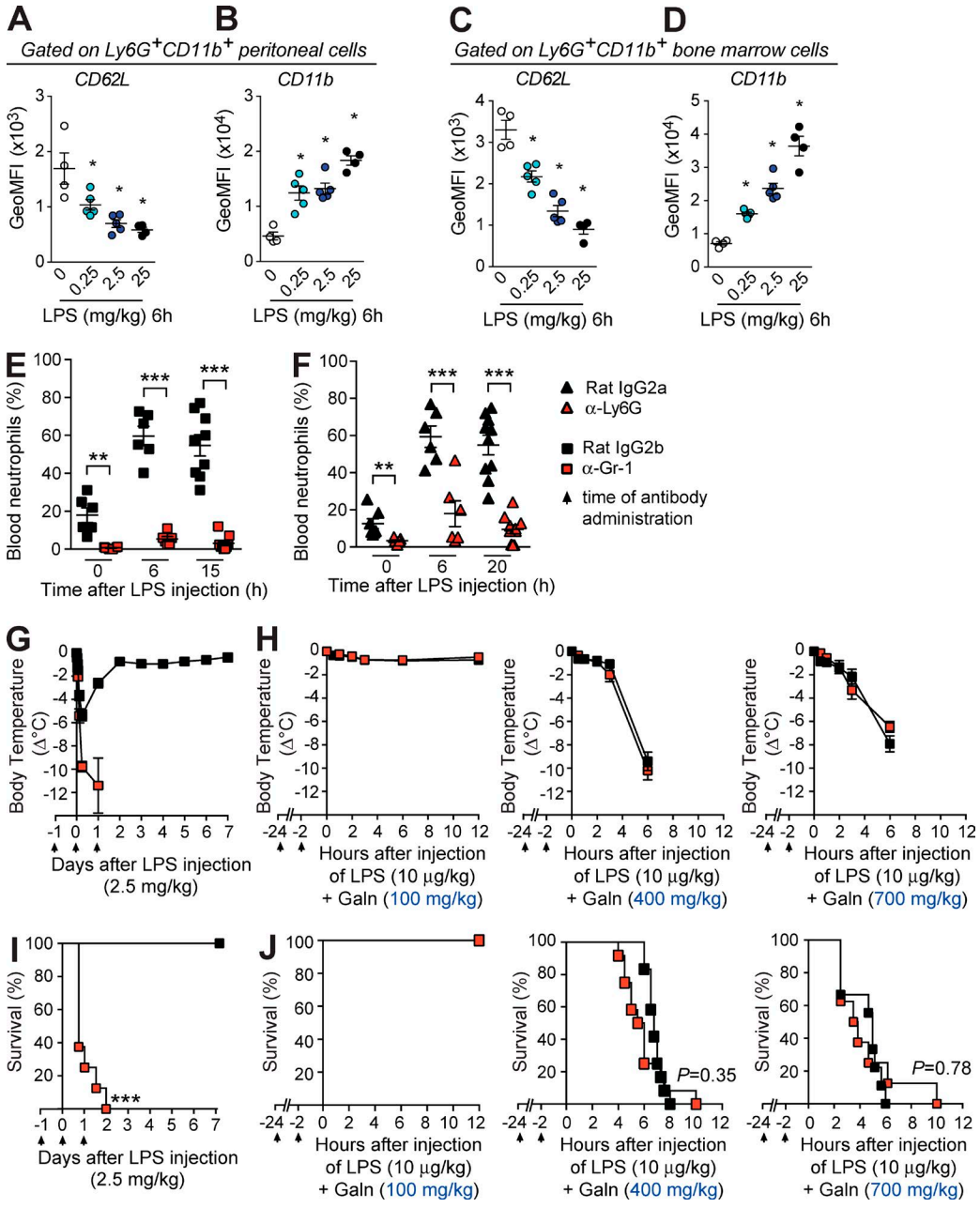

Figure S1. **Phenotype of neutrophils in the peritoneum and BM after LPS injection, and effect of treatment with neutrophil-depleting antibodies in models of LPS- or LPS/D-galactosamine–induced endotoxemia.** (A–D) Levels of CD62L (A and C) and CD11b (B and D; depicted as geometric mean fluorescence intensity [GeoMFI]) on Ly6G$^+$ CD11b$^+$ peritoneal (A and B) or BM (C and D) neutrophils 6 h after injection of various concentrations of LPS (as indicated). Results in A–D show values from individual mice; bars indicate means ± SEM pooled from two independent experiments (total n = 4–5/group). *, $P < 0.05$ versus control 0 group by two-tailed Mann–Whitney U test. (E and F) Percentage of Gr-1^{high} CD11b$^+$ blood neutrophils at the indicated time point after injection of 25 mg/kg LPS in C57BL/6J mice treated i.p. with an anti-Ly6G neutrophil-depleting antibody (clone 1A8; 500 µg/injection) or an isotype control antibody (rat IgG2a; E) and in C57BL/6J mice treated i.p. with an anti-Gr-1 neutrophil-depleting antibody (clone RB6-8C5; 300 µg/injection) or an isotype control antibody (rat IgG2b; F). Data in E and F are pooled from three independent experiments (total n = 10–12/group). **, $P < 0.01$; ***, $P < 0.001$ versus the corresponding isotype control group by two-tailed Mann–Whitney U test. (G–J) Changes in body temperature (Δ°C [mean ± SEM]; G and H) and survival (percentage of live animals; I and J) after injection of 2.5 mg/kg LPS (G and I) or 10 µg/kg LPS together with the indicated concentration of D-galactosamine (Galn; H and J) in C57BL/6J mice treated i.p. with an anti-Gr-1 neutrophil-depleting antibody (clone RB6-8C5; 300 µg/injection) or an isotype control antibody (rat IgG2b). Data in G–J are pooled from two or three independent experiments (total n = 8–12/group). ***, $P < 0.001$ versus the corresponding isotype control group by Mantel–Cox log-rank test. Arrows in G–J indicate time of i.p. injection of the neutrophil-depleting or isotype control antibodies.

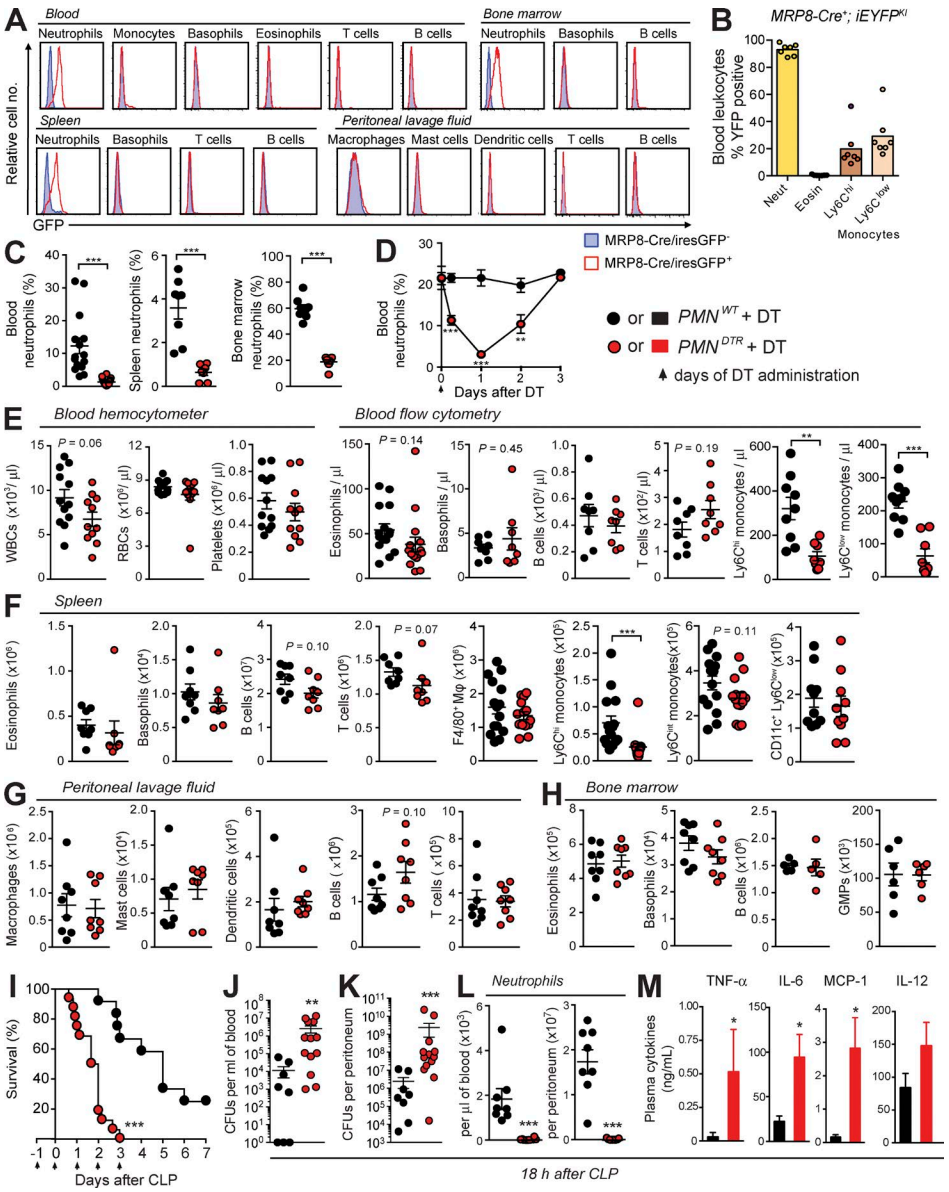

Figure S2. **Analysis of GFP expression in various immune cell types from *MRP8-Cre/IRES-GFP* mice, levels of various cell populations 24 h after DT injection into *PMN^{DTR}* mice, and responses of *PMN^{DTR}* mice in the CLP model of polymicrobial sepsis.** (A) Analysis of GFP expression (mean fluorescence intensity) in the indicated cell populations in *MRP8-Cre/IRES-GFP*$^-$ and *MRP8-Cre/IRES-GFP*$^+$ mice. Results are representative of three independent experiments. (B) Analysis of YFP expression in myeloid leukocytes from the blood of *MRP8-Cre/IRES-GFP*$^+$ × ROSA-iEYFP^{KI} reporter mice, graphed as percentage YFP$^+$ of the indicated populations. Values from individual mice are shown; bars indicate means pooled from two independent experiments (total $n = 7$). Neut, neutrophils; Eosin, eosinophils. (C) Percentage of blood, spleen, and BM neutrophils 24 h after i.p. injection of 500 ng DT into *PMN^{DTR}* mice and *PMN^{WT}* littermate control mice. (D) Percentage of blood neutrophils at the indicated time points after i.p. injection of DT on day 0. Results in D are means ± SEM from $n = 3$–8 mice per group pooled from two or three independent experiments. (E–H) Numbers of various cell populations in blood (E), spleen (F), peritoneal lavage fluid (G), and BM (H) from *PMN^{DTR}* mice and *PMN^{WT}* littermate control mice 24 h after i.p. injection of 500 ng DT, determined by hemocytometer measurements or flow cytometry. Results in C and E–H show values from individual mice; bars indicate means ± SEM pooled from two independent experiments for blood monocytes and spleen monocyte-derived DCs (moDCs; CD11b$^+$CD11c$^+$Ly6C^{low}; total $n = 8$–10/group) and BM B cells (total $n = 5$/group), four experiments for blood neutrophils (B; total $n = 15$–16/group), or three independent experiments for all other cell populations (total $n = 7$–15/group). P-values <0.3 are indicated (two-tailed Mann–Whitney *U* test). WBCs, white blood cells; RBCs, red blood cells; Mϕ, macrophages. (I–M) Responses of DT-treated *PMN^{DTR}* versus *PMN^{WT}* mice in the CLP model of polymicrobial sepsis. (I) Survival after CLP ($n = 12$–16). (J–L) Numbers of bacterial CFUs in the blood (J) and peritoneal lavage fluid (K) and numbers of blood and peritoneal neutrophils (L) 18 h after CLP ($n = 8$–13/group). (M) Levels of TNF-α, IL-6, MCP-1, and IL-12 in the plasma 18 h after CLP ($n = 7$–8/group). Results in J–L show values from individual mice; bars indicate means ± SEM; results in M are means + SEM. Data in I–M are pooled from three independent experiments. *, $P < 0.05$; **, $P < 0.01$; ***, $P < 0.001$ versus *PMN^{WT}* group by Mantel–Cox log-rank test (I) or Mann–Whitney *U* test (J–M). Arrows in D and I indicate days of i.p. injection of the neutrophil-depleting or isotype control antibodies.

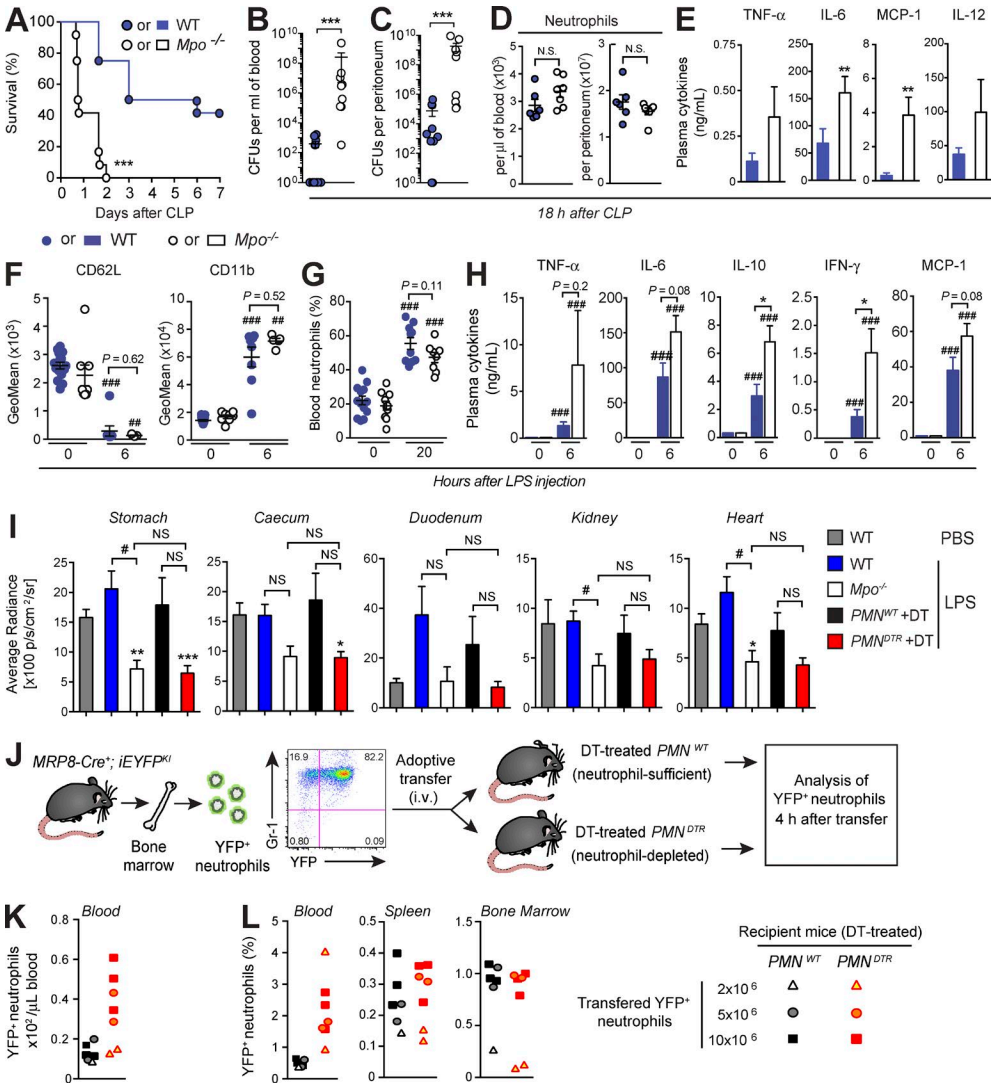

Figure S3. **Responses of MPO-deficient mice in models of polymicrobial sepsis and LPS-induced endotoxemia, systemic quantification of MPO-induced bioluminescence, and levels of neutrophils after adoptive transfer in *PMN*^{WT} versus *PMN*^{DTR} mice.** (A–E) Responses of *Mpo*$^{-/-}$ versus WT mice in the CLP model of polymicrobial sepsis. (A) Survival after CLP (n = 12). (B–E) Numbers of bacterial CFUs in the blood (B) and peritoneal lavage fluid (C; n = 9–11/group), numbers of blood and peritoneal neutrophils (D; n = 6–7/group), and levels of TNF-α, IL-6, MCP-1, and IL-12 in the plasma 18 h after CLP (n = 9–11/group). Results in B–D show values from individual mice; bars indicate means ± SEM; results in E are means + SEM. Data in A–E are pooled from two (D) or three (A–C and E) independent experiments. **, P < 0.01; ***, P < 0.001 versus WT group by Mantel–Cox log-rank test (A) or Mann–Whitney U test (B–E). (F) Quantification of CD62L and CD11b levels (geometric mean fluorescence intensity [GeoMean]) on Ly6G$^+$ CD11b$^+$ blood neutrophils before (time 0) or 6 h after injection of LPS in WT or *Mpo*$^{-/-}$ mice. (G) Percentage of blood neutrophils before (time 0) and 20 h after LPS injection (25 mg/kg) in WT and *Mpo*$^{-/-}$ mice. F and G show values from individual mice; bars indicate means ± SEM pooled from two (F) or three (G) independent experiments (total n = 5–15/group). (H) Levels of TNF-α, IL-6, IL-10, IFN-γ, and MCP-1 in the plasma of WT and *Mpo*$^{-/-}$ mice before (time 0) and 6 h after LPS injection. Data in H are means + SEM (total n = 8–12/group from three independent experiments). *, P < 0.05 versus WT group and $^{\#\#}$, P < 0.01; $^{\#\#\#}$, P < 0.001 versus the same group at time 0 by Mann–Whitney U test. (I) Quantification of MPO-induced bioluminescence in the stomach, cecum, duodenum, kidney, and heart 6 h after i.p. injection of PBS (in WT mice) or LPS (25 mg/kg) in WT mice, *Mpo*$^{-/-}$ mice, DT-treated *PMN*^{DTR} mice, and DT-treated *PMN*^{WT} littermate controls, and 5 min after luminol injection. Data are means + SEM from three independent experiments (total n = 6–14/group) except for *Mpo*$^{-/-}$ mice (two independent experiments with a total of three to four mice). *, P < 0.05; **, P < 0.01; ***, P < 0.001 versus PBS-treated WT group, and $^{\#}$, P < 0.05 versus corresponding LPS-treated control group by unpaired Student's t test. N.S., not significant (P > 0.05). (J–L) Levels of neutrophils after adoptive transfer into DT-treated *PMN*^{DTR} or *PMN*^{WT} mice. (J) Experimental outline. We purified BM neutrophils by negative selection using a commercially available kit. Purified cells were >95% Gr-1$^+$ CD11b$^+$ (as shown in J) and >90% Ly6G$^+$ CD11b$^+$ (not depicted) on average for all adoptive transfer experiments (Fig. 3 and panels K and L). Cells were >80% YFP$^+$ on average for all adoptive transfer experiments (K and L). Various numbers of purified neutrophils were transferred i.v. into DT-treated *PMN*^{DTR} mice (in which endogenous YFP$^-$ neutrophils were depleted) or DT-treated *PMN*^{DTR} mice (which contained endogenous YFP$^-$ neutrophils). 4 h after adoptive transfer, levels of YFP$^+$ neutrophils (Ly6G$^+$ CD11b$^+$) were analyzed by flow cytometry in the blood (K and L), spleen and BM (L).